

In Vivo Monitoring of Hepatic Glutathione in Anesthetized Rats by ^{13}C NMR

Jeffrey M. Macdonald,¹ Olga Schmidlin,² and Thomas L. James^{1,3*}

A method for in vivo ^{13}C NMR monitoring of hepatic glutathione (GSH) in intact, anesthetized rats has been developed. Studies were conducted using a triple-tuned, surgically implanted surface coil designed for this animal model. The coil permitted complete decoupling and sufficient resolution in the ^{13}C NMR spectrum to monitor the time course of hepatic ^{13}C -metabolites of intravenously administered 2- ^{13}C -glycine, particularly GSH at 44.2 ppm and serine signals at 61.1 and 57.2 ppm, respectively. It further allowed concomitant monitoring of high-energy phosphagens and intracellular pH by ^{31}P NMR. To confirm in vivo NMR peak assignments, we compared high-resolution 2D $^1\text{H}\{^{13}\text{C}\}$ heteronuclear multiple quantum coherence and 1D ^{13}C spectra of hepatic perchloric acid extracts to those of authentic standards. The fractional isotopic enrichment of hepatic ^{13}C -glycine increased exponentially at a rate of 1.68 h^{-1} and reached its plateau level of 81% in 2 h. The ^{13}C fractional isotopic enrichment of GSH increased exponentially at a rate of 0.316 h^{-1} and reached 55% after 4 h of 2- ^{13}C -glycine infusion, but without achieving a plateau. To confirm that the resonance at 44.2 ppm resulted from GSH, a rat was given an intravenous dose of 2-oxothiazolidine-4-carboxylic acid (OTC), a cysteine precursor that increases intracellular GSH. As expected, with OTC administration the hepatic ^{13}C GSH-to-glycine peak area increased more than sevenfold. *Magn Reson Med* 48:430–439, 2002. © 2002 Wiley-Liss, Inc.

Key words: hepatic glutathione; 2- ^{13}C -glycine; in vivo ^{13}C ; in vivo ^{31}P NMR; 2-oxothiazolidine-4-carboxylate

Glutathione (GSH) is the central antioxidant in the liver. It protects against electrophilic xenobiotics and oxidative stress by reacting with hydrogen peroxide and organic peroxides (1), and plays a central role in redox signaling (2,3). A low ratio of reduced GSH-to-oxidized glutathione (GSSG) is a critical determinant of cell death by apoptosis or necrosis (4,5). The tripeptide GSH (γ -glutamyl-cysteinyl-glycine) is synthesized by two sequential enzymatic reactions and is degraded by the GSH-dependent trans-

porter, γ -glutamyl-transpeptidase (γ -GT) (1,6). Because of its central role in hepatic metabolism (6,7), monitoring of GSH by in vivo ^{13}C nuclear magnetic resonance (NMR) spectroscopy may provide important information on the functional status of the liver, especially under pathologic conditions such as exposure to hepatotoxins, ischemia, or disease (8–10). Although its hepatic concentration (ca. 8 mM in normal rats (7)) makes GSH amenable to detection by in vivo ^{13}C NMR spectroscopy, to date there have been no reports that it has been successfully monitored in the in vivo liver.

Observation of NMR signals in intact liver is impeded by respiratory motion, magnetic susceptibility effects, and short spin-spin relaxation (T_2) times due to high concentrations of paramagnetic species, all of which lead to low spectral resolution. To overcome some of these problems, we developed a triple-tuned NMR surface coil that can be implanted in the abdominal cavity of anesthetized rats. The coil permits concomitant monitoring of GSH by ^{13}C NMR spectroscopy, and bioenergetics and intracellular pH by ^{31}P NMR spectroscopy. A ^{13}C -labeled GSH constituent, 2- ^{13}C -glycine, was infused to enrich the fraction of ^{13}C relative to ^{12}C in GSH. The level of fractional isotopic enrichment was monitored over a period of 4 h, and peak-area ratios (PARs) of sequential in vivo spectra were used to assess the turnover rate of GSH.

MATERIALS AND METHODS

Glycine (99% 2- ^{13}C -labeled) was purchased from Isotec, Inc. (Miami, OH), pentobarbital from Anthony Products (Arcadia, CA), and 50% dextrose and saline solutions from Abbott Labs (Chicago, IL). GSH, GSSG, mannitol, perchloric acid (PCA), potassium hydroxide, choline, N-dimethylglycine, betaine, sarcosine, γ -glu, cysgly, L-serine, 3-phosphoglycerate, oxalic acid, L-cysteine, L-glutamic acid, L-glutamine, L-aspartic acid, lactic acid, glucose, cystathionine, guanine, adenine, creatinine, urea, adenosine-5'-diphosphate, HPLC grade water and acetonitrile, glacial acetic acid, sodium borohydride, monobromobimane, chelex-100, and 2-oxothiazolidine-4-carboxylic acid (OTC) were obtained from Sigma Chemical Co. (St. Louis, MO), and 99.96% deuterium oxide (D_2O) was obtained from Aldrich (Milwaukee, WI). Octadecyl solid phase extraction cartridges were obtained from VWR Scientific, Inc. (Burdick and Jackson, Muskegon, MI). Bilirubin, biliverdin, and protoporphyrin were gifts from Dr. A. McDonnagh.

We constructed a coaxial, dual-slotted surface coil with single- and double-tuned circuits. The coil was photo-

¹Department of Pharmaceutical Chemistry, University of California–San Francisco, San Francisco, California.

²Department of Medicine, University of California–San Francisco, San Francisco, California.

³Department of Radiology, University of California–San Francisco, San Francisco, California.

Grant sponsor: University of California Toxic Substances Research and Teaching Program; Grant number: R01 DK52851.

Jeffrey M. Macdonald's present address is Department of Biomedical Engineering, University of North Carolina, Chapel Hill, NC 27599-7038.

*Correspondence to: Thomas L. James, Department of Pharmaceutical Chemistry, University of California–San Francisco, San Francisco, CA 94143-0446. E-mail: james@picasso.ucsf.edu

Received 30 October 2002; revised 26 April 2002; accepted 30 April 2002.

DOI 10.1002/mrm.10244

Published online in Wiley InterScience (www.interscience.wiley.com).

© 2002 Wiley-Liss, Inc.

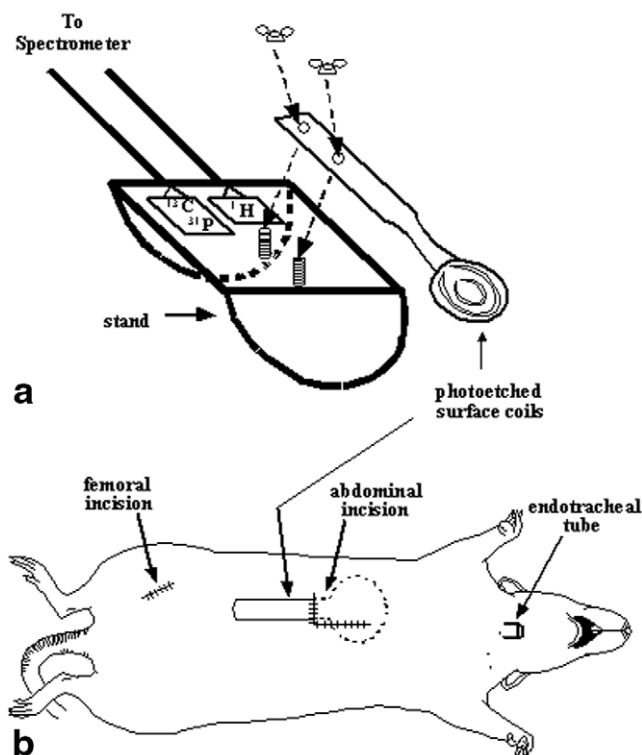


FIG. 1. Schematic representation of (a) the coaxial dual-slotted photo-etched surface coil and plastic stand, and (b) the surface coil implant in a rat. After the surface coil is implanted, it is connected to the matching and tuning circuit on the stand and the assembly is placed in a cradle, which is then inserted into the magnet.

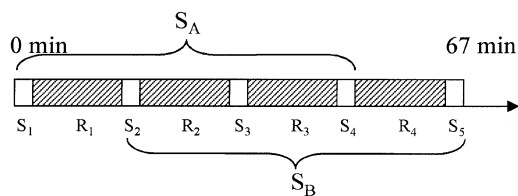
etched onto an ultraviolet-sensitive circuit board (11) and made rigid with epoxy and fiberglass. The outside coil (24 mm diameter) was single-tuned to the ^1H frequency (200.11 MHz), and the inside coil (13 mm diameter) was connected to a balance-matched, double-tuned $^{13}\text{C}/^{31}\text{P}$ circuit (Fig. 1a) (12). A glass sphere containing 40% dioxane was placed in the center of the surface coil as a reference.

All animal studies were approved by the Committee on Animal Research, University of California–San Francisco. For in vivo NMR studies, six female Sprague-Dawley rats (240–260 g) were anesthetized with pentobarbital ($50 \text{ mg} \cdot \text{kg}^{-1}$ via intraperitoneal injection). The femoral artery and vein were cannulated with PE-50 tubing for blood pressure and blood gas monitoring, as well as fluid and drug infusion. The rats were mechanically ventilated through a tracheal tube. The NMR coil was inserted in the peritoneal cavity through an L-shaped abdominal incision and placed above the liver (Fig. 1b). This was done in a similar fashion to the first hepatic studies with implanted coils in rats (13). The rats were placed on a cradle in a supine position. To reduce coil motion and ensure reproducible placement, the coil was bolted to a plastic stand (Fig. 1a). The rats received a continuous intravenous (i.v.) infusion of 10% glucose, 4% mannitol, and $20 \text{ mg} \cdot \text{kg}^{-1} \cdot \text{h}^{-1}$ pentobarbital at a rate of 3 mL/hr for 1.5 h. After baseline spectra were obtained, one of two protocols was followed in monitoring hepatic levels of ^{13}C -GSH: 1) $2\text{-}^{13}\text{C}$ -glycine at a dose of $4.4 \text{ mmol} \cdot \text{kg}^{-1} \cdot \text{h}^{-1}$ was added to the above infusate, and

the infusion was continued for 4 h ($N = 5$); 2) the same protocol was used, but 1 h after start of the glycine infusion, $15 \text{ mmol} \cdot \text{kg}^{-1}$ of OTC was infused intravenously over 0.5 h ($N = 1$). The time from coil implantation to euthanization was 6 h.

Within 5 min of completing the in vivo experiment, livers were excised and immediately frozen in liquid N_2 . The actual dissection lasted less than 10 s. PCA extracts of liver tissue were prepared by a modification of previously described methods (14). Briefly, mortar and pestle under constant liquid N_2 were used to pulverize the livers. PCA 0.6N (6%) was added at a volume-to-weight ratio of 2:1. The mixture was then placed on ice in a centrifuge tube until thawed. The cell mass was pelleted by centrifugation at 15000 rpm for 10 min. The supernatant was titrated to pH 7.4 with KOH, centrifuged (15000 rpm for 10 min) to pellet the perchlorate salts, frozen in liquid N_2 , and lyophilized. For analysis by high-resolution NMR, samples were titrated to the appropriate pH with NaOD, treated with Chelex-100 to remove paramagnetic ions, re-lyophilized, and dissolved in 100% D_2O . For identification of amides by the deuterium isotope shifts (15,16), a mixture of D_2O : H_2O was used to dissolve the liver extracts. Additional PCA extracts, subsequently referred to as “bench-top studies,” were obtained to determine the fractional enrichment (FE) of ^{13}C in glycine and its metabolites (see below). These studies were performed using protocol 1 as described above, except that rats were not placed in the magnet, and the implanted coil was not pulsed. All lyophilized samples were stored at 0°C until NMR spectroscopic analysis.

In vivo spectroscopic experiments were performed using a Nalorac Cryogenics Corporation (Martinez, CA) Quest 4400 NMR imaging spectrometer connected to a 4.7 Tesla horizontal bore (16 cm usable bore) Oxford magnet. The ^1H coil was used to optimize the static magnetic field homogeneity by shimming on the $^1\text{H}_2\text{O}$ proton resonance, using a 90° flip angle, until a water proton line-width in the range of 50–80 Hz was obtained. The in-plane 180° pulses for ^1H , ^{13}C , and ^{31}P were calibrated using a microsphere containing 2M $2\text{-}^{13}\text{C}$ -glycine and 5% phosphoric acid. The in-plane 90° pulse for ^{13}C was determined at the beginning of each experiment using 40% dioxane. ^{13}C spectra were obtained at 50.3 MHz with decoupling of protons during acquisition and quadrature phase detection. Even though the ^1H coil was well insulated with epoxy, to avoid local heating of the liver, sensitivity gain via the nuclear Overhauser effect with continuous proton irradiation was not attempted (17). Partially relaxed spectra were obtained from 144 transients with a 70° in-plane flip angle, 2K data points, a sweep width of $\pm 4443 \text{ Hz}$, and a repetition time (TR) of 1 s, yielding a total acquisition time of 9.6 min. A 70° in-plane flip angle was chosen because it yielded an optimal signal-to-noise ratio and provided sufficient localization, as demonstrated by the lack of phosphocreatine signal in the in vivo ^{31}P NMR spectra (18). A representative in vivo hepatic ^{31}P NMR spectrum has been presented elsewhere (13,19). The ^{31}P 90° pulse was calculated from the in-plane in vivo ^{13}C 90° pulse length. The calculation was based on the difference between the ^{31}P and ^{13}C in-plane 90° pulse lengths obtained from standards. ^{31}P spectra were obtained at



SCHEME 1.

81 MHz using a one-pulse sequence, with the same parameters as described above except the TR was 1.2 s with 100 transients, yielding a total acquisition time of 8.8 min. Two or three ^{31}P spectra were summed for peak area determination. Three ^{13}C and ^{31}P spectra were obtained sequentially. Prior to Fourier transformation, time domain ^{13}C and ^{31}P data were processed with Gaussian (16–22 Hz) and exponential (25–50 Hz) apodization, respectively. The ^{13}C and ^{31}P spectra were plotted and referenced to dioxane and α -NTP at 68.0 and -7.5 ppm, respectively. GSH and glycine were also identified *in vivo* by determining the C-H coupling constant in a coupled spectrum.

In two additional *in vivo* experiments, performed according to protocol 1 (see above), saturation factors (SFs) of GSH, glycine, serine C2, serine C3, and dioxane were determined. The same NMR parameters were used as described above. Over a period of 4 h, consecutive sets of saturated (S_i) and relaxed (R_i) *in vivo* ^{13}C spectra were obtained from 40 transients each, with TRs of 1 and 5 s, respectively, and acquisition times of 2.67 and 13.33 min, respectively (as shown in Scheme 1). The spin-lattice relaxation time (T_1) values of [2- ^{13}C -glycyl]glutathione in red blood cells have been reported to range from 0.84 s to 0.92 s (20). Consequently, a TR of 5 s was considered sufficient to achieve full relaxation, as relaxation in the liver should be at least as rapid as in red blood cells. SFs were calculated according to Eq. [1] as the ratio of the relaxed-to-saturated peak areas. For GSH, a single SF was calculated using five saturated and four relaxed spectra obtained between 170 and 237 min of glycine infusion when ^{13}C -glycine enrichment had reached a plateau. For all other compounds, consecutive SF values were calculated and found to be constant with time.

$$\begin{aligned} R &= R_1 + R_2 + R_3 + R_4 \\ S_A &= S_1 + S_2 + S_3 + S_4 \\ S_B &= S_2 + S_3 + S_4 + S_5 \\ SF &= 2R/(S_A + S_B) \end{aligned} \quad [1]$$

1D NMR spectra of liver extracts dissolved in D_2O were obtained using a GE QE-300 (^{13}C , ^{31}P , ^1H) spectrometer operating at a ^1H frequency of 300 MHz. ^{13}C and ^{31}P spectra were obtained using a one-pulse sequence with decoupling during acquisition, a 10-s interpulse delay, 16K complex points, and a spectral width of ± 10000 Hz (^{13}C) or ± 4000 Hz (^{31}P). Prior to Fourier transformation, time domain transients were zero-filled and processed with a negative Lorentzian-to-positive Gaussian transformation for resolution enhancement, which is useful in determining coupling constants. ^{13}C and ^{31}P compounds

were identified by comparison of extract chemical shifts and CH coupling constants to those of known standards, literature values, and known glycine biochemical pathways. GSH was further identified by its *in vivo* ^{13}C coupling constant, the deuterium-isotope shift (15,16), and by addition of known amounts of GSH and GSSG to liver extracts. ^{13}C and ^1H spectra were referenced to 3-(trimethylsilyl)propionic-2,2,3,3- d_4 acid at -2 and 0 ppm, respectively. ^{31}P spectra were referenced to the α -nucleotide triphosphate (NTP) peak at -7.5 ppm, and the intracellular pH was determined using the chemical shift of inorganic phosphate relative to α -NTP (21).

^{13}C -labeled glycine metabolites in liver extracts were also identified by 2D $^1\text{H}\{^{13}\text{C}\}$ heteronuclear multiple quantum coherence (HMQC) spectroscopy using a Varian (Palo Alto, CA) UNITY Plus 500 MHz NMR spectrometer. The HMQC spectra were obtained with a 5-mm Nalorac triple resonance probe, and using a spectral width of 6518.9 Hz and 2048 complex data points, yielding an acquisition time of 0.314 s. The HMQC pulse sequence entailed ^{13}C GARP1 decoupling during acquisition, interpulse delay of 0.38 s, scalar evolution delay of 71 ms, and 1 s presaturation pulse. The t1 dimension had a spectral width of 12500 Hz and 640 increments and was collected in phase-sensitive mode. 2D spectra were zero-filled to 4096 in t1, and apodization consisted of a shifted sine-bell function.

FE of ^{13}C in glycine and GSH was determined in PCA extracts from ^1H one-pulse spectra, by comparing the ^{13}C -coupled (i.e., from ^{13}C satellite peaks) and ^{12}C -uncoupled peak areas (22). FE of glycine was determined at 1 and 2 h in liver extracts from bench-top studies ($N = 3$, each) and at 4 h in extracts from both *in vivo* ($N = 5$) and bench-top studies ($N = 3$). FE of GSH was determined in liver extracts from bench-top studies ($N = 3$ each at 1, 2, and 4 h) as described by Gamcsik (23) with slight modification. Briefly, 100 mg of lyophilized liver extract was dissolved in 50 mM HCl-TRIS, and 50 mM sodium borohydride was added to reduce GSSG to GSH. After 1 h of incubation at 37°C , 100 mM of monobromobimane was added, and the extracts were left overnight at 20°C to react in darkness. The resulting GS-bimane (GSBi) was purified from extracts with octadecyl solid phase cartridges as described by Gamcsik (23). To remove hydrophobic macromolecules, GSBi extracts were further purified by a second extraction with octadecyl solid phase cartridges by loading samples with 99% H_2O with 1% acetic acid (pH 2.9) and eluting with 100% H_2O (pH 7.0). ^1H NMR spectra of GSBi extracts were obtained between pD 3.75 and 4.5 to maximize the chemical shift separation between the [α -glycyl]GSH and [α -glutamyl]GSH resonances. With a Varian UNITY Plus 500 MHz NMR spectrometer, a one-pulse sequence was used with a 45° flip angle, 10-s interpulse delay, 16K complex points, and a spectral width of ± 3012 Hz. The [α -glycyl]GSH FE was calculated as the ^{13}C -coupled satellite peak area divided by the ^{13}C -coupled satellite peak area plus ^{12}C -uncoupled peak area.

Peak areas were fit using the "MacFID" software package (Tecmag, Inc., Houston, TX), and GSH FE was determined from peak area integration using "VNMR" software, v. 6.01 (Varian, Inc.). Within each *in vivo* spectrum, the GSH and glycine peak areas were referenced to the dioxane peak area. For kinetic analysis, the *in vivo* PARs of gly-

cine-to-dioxane and GSH-to-dioxane were used to construct FE vs. time plots. The glycine-to-dioxane PAR at 4 h, in each of the five in vivo experiments, was set equal to the FE of glycine determined in the hepatic extract of the respective experiment. The GSH-to-dioxane PARs at 4 h were set to the average FE of GSH, 55%, determined from the three bench-top studies at 4 h. For all remaining time-points of the in vivo studies, the PARs were converted proportionally to estimated values of FE by using the following equation: $FE_{tn} = (FE_{t4} * PAR_{tn}) / PAR_{t4}$, where FE_{tn} and FE_{t4} are the FEs at time n and at 4 h, respectively, and PAR_{tn} and PAR_{t4} are the PARs at time n and at 4 h, respectively.

Differences between mean glycine FE levels in hepatic extracts from in vivo ($N = 5$) and bench-top studies (4 h time-point; $N = 3$) were compared with an unpaired *t*-test using StatView 5 statistical software (SAS Institute, Inc., Cary, NC) and were considered to be significant if $P < 0.05$. Turnover rate constants (*k*) of glycine and GSH were calculated from the time course of in vivo FE values (vide supra) by least-squares fitting of an exponential function using the "Regression" software package, v. M1.23 (Blackwell Scientific Publications, UK). Saturation factors were fit with the same software using the equation $y = ax + b$, and were considered linear if $r^2 > 0.95$. Results are reported as mean \pm standard error of the mean.

RESULTS

The major findings outlined below demonstrate that we can continuously monitor in vivo hepatic glutathione levels via ^{13}C NMR using a newly developed triple-tuned, implanted surface coil in anesthetized rats. The rat liver retains viability in spite of the presence of the implanted coil. Observation of glutathione, as well as administered glycine, enables turnover rates for these metabolites to be estimated.

Viability of In Situ Liver in the Presence of the Implanted Surface Coil

As assessed by in vivo ^{31}P NMR, hepatic NTP did not change significantly. The percent of β -NTP peak area to total phosphate signal was $18.1\% \pm 1.7\%$ at baseline, and $17.7\% \pm 2.6\%$ after 3.5 h of $2\text{-}^{13}\text{C}$ -glycine infusion. In all rats, hepatic pH remained stable at values of 7.30 ± 0.04 throughout the course of the experiment. These results indicate that glycine infusion and continuous anesthesia and mechanical ventilation did not significantly alter bioenergetics over the course of 4 h. However, since the bioenergetic status of the liver was not determined in both the absence and the presence of the implanted NMR coil, it is not clear whether implantation of the coil itself may have altered that status.

Detection and Identification of ^{13}C Metabolites

In baseline in vivo spectra (Fig. 2a, bottom spectrum) no distinct signal from naturally abundant ^{13}C was detectable. Continuous i.v. infusion of $2\text{-}^{13}\text{C}$ -glycine resulted in ^{13}C NMR signals in the liver from labeled glycine (42.4 ppm) within 10 min of the start of the infusion (Fig. 2a, second

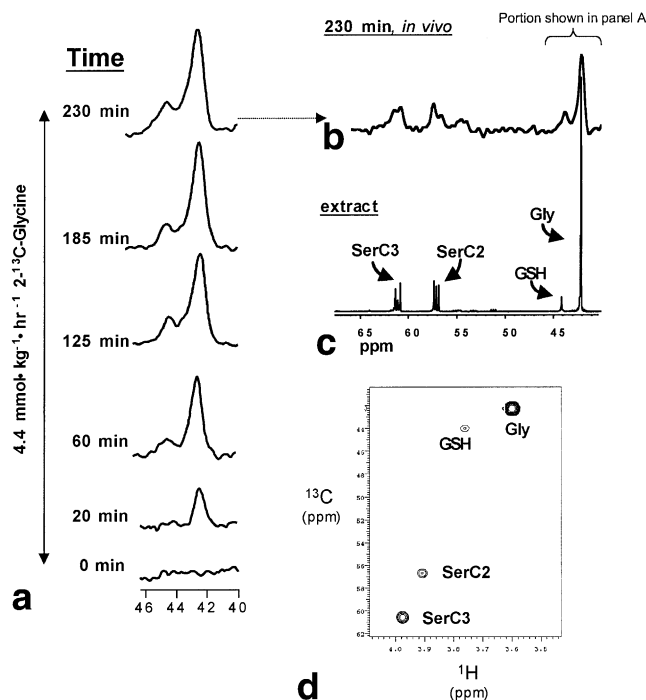


FIG. 2. **a**: A representative series of hepatic in vivo ^{13}C spectra obtained before and during 230 min of $2\text{-}^{13}\text{C}$ -glycine infusion, $4.4 \text{ mmol} \cdot \text{kg}^{-1} \cdot \text{h}^{-1}$, showing the time course of glycine and GSH resonances. **b**: A larger portion of the topmost spectrum shown in panel a (230-min time-point). **c**: The ^{13}C spectrum of the hepatic extract from the same rat (pH 7.4; 25°C). The $^1\text{H}\{^{13}\text{C}\}$ -HMQC spectrum in panel d was obtained from the same hepatic extract as shown in panel c, and was used to identify the ^{13}C -labeled compounds. **a** and **b**: In vivo spectra are composed of 144 acquisitions obtained in 9.6 min. **c**: The hepatic extract spectrum is composed of 5000 acquisitions with a TR of 11 s. Abbreviations: SerC2, C2 serine; SerC3, C3 serine; GSH, glutathione; Gly, glycine.

spectrum from bottom). The resonance resulting from labeled glycine was the most prominent resonance other than that from dioxane, the external standard (68 ppm, not shown in the figures). The resonance at 44.2 ppm, which appeared within 20 min (Fig. 2a, third spectrum from bottom), was identified as GSH. A pair of resonances, also appearing within 20 min after the start of the $2\text{-}^{13}\text{C}$ -glycine infusion, were identified as serine C2 and C3 centered at 57.2 ppm and 61.1 ppm, respectively. The series of ^{13}C spectra in Fig. 2a illustrates that during the entire experiment the peak areas of GSH and glycine are sufficiently resolved to be quantified employing a standard peak area fitting program.

In addition to utilizing ^{13}C and ^1H chemical shifts (Fig. 2c and d) (24), we identified GSH by its coupling constant both in vivo and in hepatic extracts, and by its deuterium isotope-induced ^{13}C shift in hepatic extracts (Fig. 3b, inset). The coupling constant and isotope shift were 139.2 Hz and 0.11 ppm, respectively, and identical to those of a sample of authentic GSH. These parameter values are typical for methylene protons coupled to an adjacent exchangeable amide proton. When exogenous GSH was added to liver extracts, it was completely oxidized to GSSG if extracts were dissolved in either H_2O or D_2O and were kept at 25°C for ≥ 48 h.

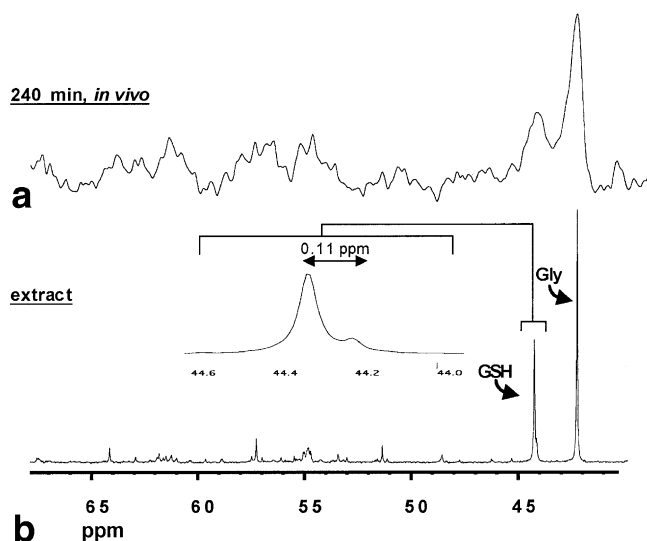


FIG. 3. **a:** The central portion of a hepatic in vivo ^{13}C NMR spectrum obtained at 240 min of $2\text{-}^{13}\text{C}$ -glycine infusion, $4.4\text{ mmol} \cdot \text{kg}^{-1} \cdot \text{h}^{-1}$, and concomitant administration of OTC, $15\text{ mmol} \cdot \text{kg}^{-1}$, during the initial 30 min of glycine infusion. **b:** The ^{13}C extract spectrum of the same liver (20% D_2O ; pH 7.4; 25°C). The inset is an enlargement of the $[2\text{-}^{13}\text{C}\text{-glycyl}]\text{GSH}$ resonance, demonstrating the deuterium isotope shift of 0.11 ppm.

To further confirm that the in vivo ^{13}C resonance at 44.2 ppm is hepatic GSH, and to explore the feasibility of experimentally enhancing the GSH signal intensity, $15\text{ mmol} \cdot \text{kg}^{-1}$ of OTC was infused i.v. for 30 min during the administration of $2\text{-}^{13}\text{C}$ -glycine. OTC is metabolized to cysteine by oxoprolinase, a cytosolic enzyme that constitutively forms glutamate from its cyclic form oxoproline (1). With the administration of OTC, the PAR of GSH-to-glycine increased by a factor of 1.8 in vivo (Fig. 3a) and by a factor of 7.6 in extracts (Fig. 3b). In contrast, OTC decreased the level of 2, 3- ^{13}C -serine. In extract spectra (Figs. 2c and d, and 3b), isotopomers of serine C3 (SerC3, 61.1 ppm) and serine C2 (SerC2, 57.2 ppm) can be identified. The serine isotopomers comprise 2- ^{13}C -serine (singlet), 3- ^{13}C -serine (singlet), and 2, 3- ^{13}C -serine (two doublets; $J_{23} = 36.6\text{ Hz}$). OTC administration increased the ^{13}C enrichment of anaerobic end-products such as lactate (69.3 ppm, not shown) and alanine (51.3 ppm). These effects are consistent with a systemic decrease in oxidative metabolism possibly due to cardiovascular or neurological toxic effects of OTC (25) and cysteine (26), respectively. The largest naturally abundant compound in the ^{13}C NMR

spectrum of the hepatic extract in Fig. 3b represents taurine (48 ppm and 36 ppm), the catabolite of OTC (27).

Visibility of NMR Signals In Vivo

To estimate the NMR visibility of signals from $2\text{-}^{13}\text{C}$ -glycine and its metabolites in vivo, we compared their PARs from in vivo spectra (Fig. 2b) with those from extract spectra (Fig. 2c) after correcting signal intensities for saturation effects (Table 1). This comparison provides an estimate of the in vivo visibility of metabolites relative to each other. To determine absolute visibility of these metabolites in vivo, further studies will be necessary using methods such as those described by Shungu et al. (28). The PARs of GSH-to-glycine, SerC2-to-glycine, SerC3-to-glycine, GSH-to-SerC2, and GSH-to-SerC3 were all smaller in extract spectra as compared to in vivo spectra. The degree by which the various PARs are decreased in extract spectra, expressed as “% difference” in Table 1, implies that the peak areas of the three major ^{13}C -labeled compounds are enhanced in the extract spectra, relative to in vivo spectra, in the following order: glycine > serine > GSH, with the relative amount of glycine being 75% larger and that of GSH being 50% smaller than that of serine in extract spectra. One possible explanation for these observations is that there are pools of glycine and perhaps serine that are not NMR-visible in vivo. Alternatively, some GSH and perhaps serine may have been lost during the extraction procedure. One other complicating factor is possible contributions from the blood volume in the liver. These are considered in the Discussion section.

Kinetics of NMR-Detectable Metabolites

The ^{13}C FE of glycine, as determined in hepatic extracts from one-pulse ^1H spectra, increased rapidly after the start of $2\text{-}^{13}\text{C}$ -glycine infusion and reached $70\% \pm 2\%$, $72\% \pm 3\%$, and $81\% \pm 1\%$ after 1, 2, and 4 h, respectively. FE of GSH, as determined in hepatic extracts from the satellite resonances of the GSBi derivative of GSH (Fig. 4), increased at a slower rate and reached $17 \pm 2\%$, $31 \pm 1\%$, and $55 \pm 1\%$ after 1, 2, and 4 h, respectively. FE values of both GSH and glycine determined experimentally in hepatic extracts did not differ significantly from their FE values derived from in vivo spectra (Fig. 5a and b). The data suggest that FE of GSH did not achieve equilibrium with glycine during the 4-hr observation period.

To assess turnover rates of GSH and glycine during $2\text{-}^{13}\text{C}$ -glycine infusion, we fitted estimated FE values (see Methods section) of each of the five in vivo experiments to a monoexponential function, $y = A(1 - e^{-kt})$ (29). For GSH,

Table 1
Peak Area Ratios of the Major ^{13}C -Labeled Compounds in Extract and In Vivo ^{13}C NMR Spectra

Peak area ratio ^a	GSH/Gly	SerC2/Gly	SerC3/Gly	GSH/SerC2	GSH/SerC3
In vivo	0.31 ± 0.03	0.44 ± 0.05	0.35 ± 0.04	0.74 ± 0.17	0.92 ± 0.09
Extract	0.12 ± 0.02	0.25 ± 0.02	0.20 ± 0.02	0.49 ± 0.05	0.63 ± 0.10
Difference, %	-61	-43	-43	-34	-32

^aPeak areas were adjusted for saturation effects. Saturation effects did not change significantly over the 4-h observation period and were as follows: dioxane, 2.25 ± 0.02 ; glycine, 1.52 ± 0.01 ; SerC2, 1.19 ± 0.02 ; SerC3, 1.02 ± 0.02 ; GSH, 1.05 ± 0.02 .

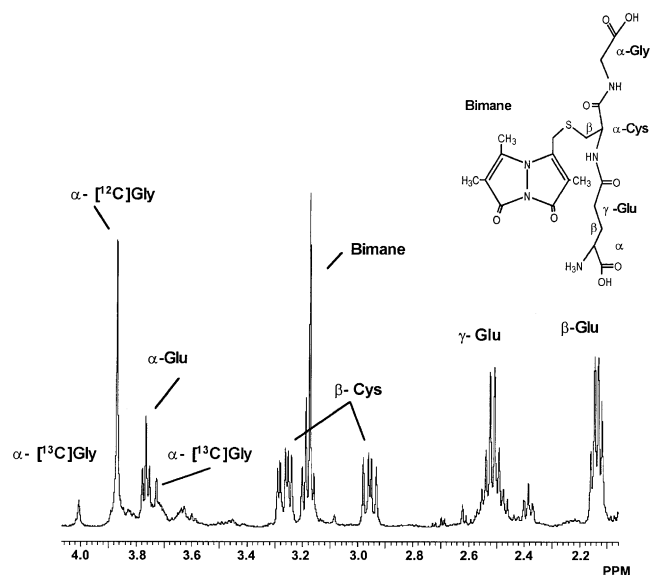


FIG. 4. Portion of the ^1H spectrum of the GSBi derivative purified from a PCA liver extract obtained 1 h after the start of $2\text{-}^{13}\text{C}$ -glycine infusion. The inset shows the structure of the GSBi derivative. In order to achieve maximal chemical shift separation between the glycyI and glutamyl satellites, ^1H spectra were obtained at a pH between 3.75 and 4.5.

the preexponential coefficient A was set equal to the experimentally determined FE value of glycine in the respective hepatic extract assuming that at steady-state, FE values of GSH and glycine will be identical. The average GSH turnover rate, k , was 0.316 ± 0.008 ($r^2 = 0.94 \pm 0.004$) corresponding to an average $t_{1/2}$ of 2.2 h. This suggests that the FE value of GSH attains its plateau approximately 11 h after the start of the $2\text{-}^{13}\text{C}$ -glycine infusion. Figure 5a shows the time course of $[\alpha\text{-}^{13}\text{C}\text{-glycyl}]\text{GSH}$ levels, expressed as % FE, in the five in vivo experiments. The time course of glycine FE levels obtained from the same experiments is shown in Fig. 5b. The glycine data were fitted using the same function as for GSH, but in this case both “ A ” and “ k ” were determined by the curve-fitting routine. The average turnover rate, k , was 1.685 ± 0.679 ($r^2 = 0.96 \pm 0.03$) corresponding to a $t_{1/2}$ of 25 min; the average A was $81.2 \pm 1.01\%$.

Both the serine C2 and C3 resonances increased proportionately over time and reached a plateau by 120 min (data not shown). Values of the SF (Eq. [1], Scheme 1) for SerC2 and SerC3 did not change significantly during $2\text{-}^{13}\text{C}$ -glycine infusion, being 1.19 ± 0.02 and 1.02 ± 0.02 , respectively. The difference between SF for SerC2 and SerC3 reflects faster spin-lattice relaxation of the α -carbon due to the additional covalently attached proton as compared to the β -carbon (30). The PAR of the SerC2-to-SerC3 resonances was 0.80 ± 0.03 in extracts after 1 h of $2\text{-}^{13}\text{C}$ -glycine infusion and did not change with time (data not shown). Comparison of the SerC2 and SerC3 resonances in Fig. 2c shows that the center line singlet intensity of the $2\text{-}^{13}\text{C}$ -serine isotopomer is twice that of the $3\text{-}^{13}\text{C}$ -serine isotopomer.

DISCUSSION

Detection of Hepatic Glutathione and Other Metabolites In Situ

Using in vivo ^{13}C NMR spectroscopy we monitored hepatic levels of GSH and other metabolites of infused $2\text{-}^{13}\text{C}$ -glycine in healthy anesthetized rats. The proximity of the glycine and GSH resonances in ^{13}C spectra made it necessary to obtain good sensitivity from the radiofrequency coil, complete decoupling, and narrow linewidths. This was accomplished by use of a specially developed triple-tuned coil in conjunction with a rigid assembly. This technique further allowed us to monitor hepatic bioenergetics and intracellular pH concomitantly via ^{31}P NMR.

Infusion of ^{13}C -glycine gave rise to major ^{13}C resonances in vivo at 42.4, 44.2, 57.2, and 61.1 ppm, which we iden-

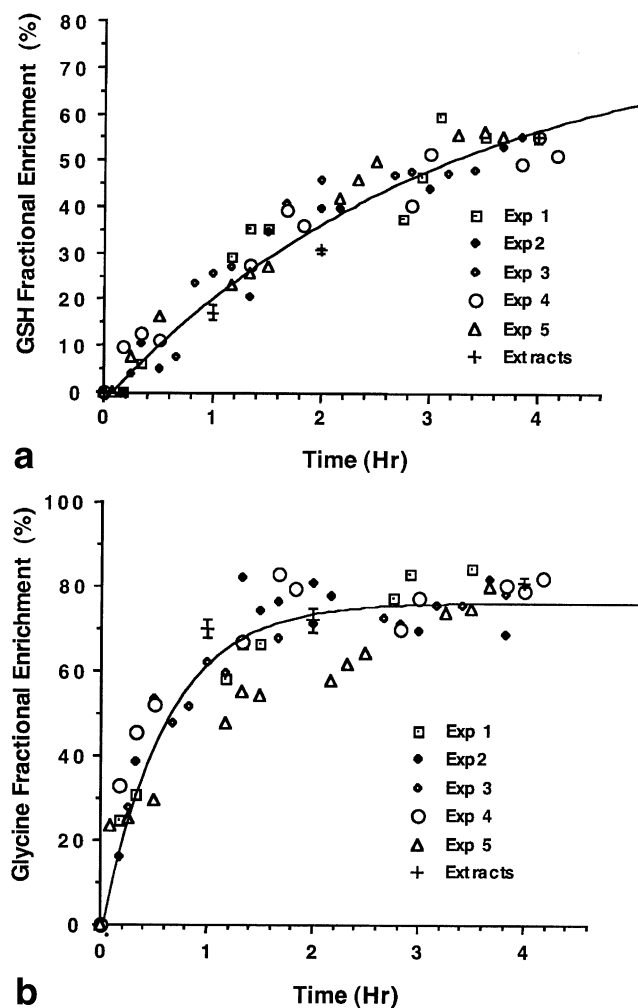


FIG. 5. Time course of (a) ^{13}C -GSH and (b) ^{13}C -glycine levels in rat liver ($N = 5$) during intravenous infusion of $2\text{-}^{13}\text{C}$ -glycine, $4.4 \text{ mmol} \cdot \text{kg}^{-1} \cdot \text{h}^{-1}$, over a maximum duration of 260 min. The plots include data from the experiment depicted in Fig. 2a (labeled “Exp 3” in this figure). Data are presented as % FE ^{13}C and were derived from in vivo spectra using PARs (for details, see Methods section). The plots also include FE levels of glycine and GSH determined experimentally in hepatic extracts at 1, 2, and 4 h (+). Data were fitted with a one-compartment model using the equation $y = A(1 - e^{-kt})$. Extract data were not included in the fits.

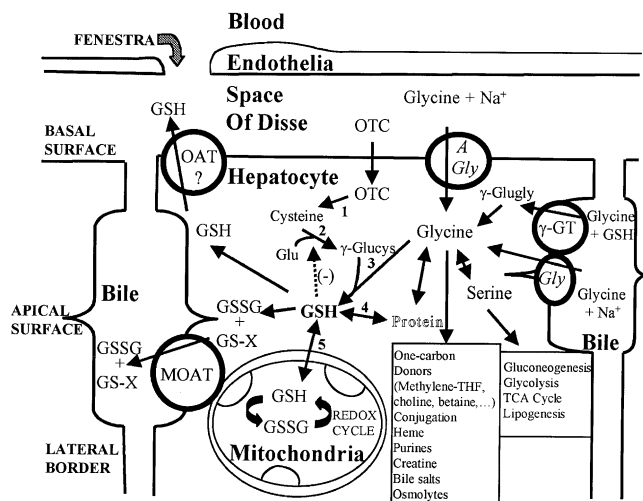


FIG. 6. Diagram depicting the hepatic transport and various metabolic pathways of glycine and GSH. Abbreviations: GSH, reduced glutathione; GSSG, oxidized glutathione; GS-X, conjugated glutathione; γ -GT, γ -glutamyl transpeptidase; TCA, tricarboxylic acid; THF, tetrahydrofolate; Gly, symporter; A, symporter; MOAT, multi-specific organic anion transporter; OAT, organic anion transporter and the ? is to represent that this is the proposed transporter of GSH efflux. Reaction 1 is catalyzed by 5-oxoprolinase; reaction 2 is catalyzed by γ -glutamylcysteine synthetase; reaction 3 is catalyzed by GSH synthetase; reaction 4 is catalyzed by thiol transferase; reaction 5: high- and low-affinity mitochondrial transporters.

tified from their chemical shifts and coupling constants, and from 2D NMR studies of hepatic extracts as glycine, GSH, and serine C2 and C3, respectively. The ^{13}C resonance at 44.2 ppm was of particular interest, since it represents GSH (24). When OTC, a cysteine precursor, which increases GSH levels (Fig. 6) (31), was infused together with 2- ^{13}C -glycine, the signal intensity at 44.2 ppm increased severalfold, as expected. Comparison of the deuterium isotope-induced shift and the coupling constant of this resonance in ^{13}C extract spectra to those produced by authentic GSH added to extracts of untreated liver showed that the two coupling constants and the two isotope shifts were identical, and thus confirmed that the resonance resulted from GSH.

Monitoring of GSH by NMR was first accomplished in human red blood cells by using ^1H NMR (32), and then in human brain via in vivo ^1H double quantum coherence (DQC) NMR (33), and in excised rat liver by using ^{13}C NMR (34). It has not been reported in liver of an intact animal (35), even though the steady-state concentration of GSH in liver is one of the highest of any organ (about 8 mM in rat (1)). Respiratory motion and high concentrations of paramagnetic cations in the liver causing short spin-spin and spin-lattice relaxation values have been major barriers to the monitoring of GSH in vivo by ^1H DQC NMR or by difference spectroscopy (22). In the current study we used 2- ^{13}C -glycine to label hepatic GSH, which is synthesized in the cytosol of the hepatocyte from glycine and γ -glu-cys, a reaction catalyzed by glutathione synthetase (reaction 3 in Fig. 6). Unlike cysteine or glutamate, glycine is not involved in any regulatory step of GSH synthesis, so infusion of glycine should have little effect on GSH homeosta-

sis (6,36). In fact, its 2- ^{13}C -isotopic label has been used previously to determine the turnover rate of GSH in hepatic extracts by mass spectroscopy (37). Further, the chemical shift of [2- ^{13}C -glycyl]GSH is in an area that is relatively free of endogenous ^{13}C NMR resonances.

NMR Visibility of Hepatic Metabolite Signals

Since we did not determine absolute metabolite concentrations in the current study, no definitive statements can be made regarding NMR visibility of metabolites. However, comparisons of the PARs of 2- ^{13}C -glycine and its metabolites in extract and in vivo spectra (Table 1) suggest that the various compounds apparently differ considerably with respect to the visibility of their in vivo NMR spectral signals. Specifically, the signal of glycine, relative to those of GSH and serine, appears reduced in vivo compared to extract spectra. This may be explained by either an apparent decrease of glycine signal in vivo or by disproportionate losses of GSH and serine during tissue extraction, or by both. An apparent decrease in glycine signal visibility in vivo may occur via blood flow effects. The liver receives about one third of cardiac output, and blood occupies 25–30% of the liver volume (38). Normally, plasma concentrations of glycine, GSH, and serine are in the micromolar range (1,39). Infusion of 4.4 mM \cdot kg \cdot h glycine will increase the plasma concentration of glycine into the millimolar range (40), but presumably it will not substantially alter plasma levels of GSH or serine. A contribution to the glycine NMR signal from blood in the liver will occur for the extracts, as the livers were not desanguinated after excision. In vivo glycine signal visibility may be reduced when, during signal acquisition, part of the RF-pulse-labeled intravascular hepatic glycine is carried by the circulating blood beyond the boundary of signal detection. The effect this has on the signal ratios of in vivo and extract spectra depends on the concentration of analyte in the blood, the RF pulse width and length of signal acquisition, and blood flow rate in the sensitive area of the NMR coil (41).

Not explained by "blood flow effects," however, are the differences between in situ and extract ratios of GSH and serine signals. The PARs imply that either some GSH was lost during PCA extraction, or a pool of serine is not visible in the intact liver. Binding of a substantial fraction of serine to macromolecular structures could decrease its in vivo NMR signal intensity. However, there has been nothing reported to suggest that occurs.

Some portion of GSH may have been lost during excision of the liver or during the extraction procedure, but care was taken to avoid this. Upon completion of in vivo studies, livers were flash frozen in liquid nitrogen without prior desanguination to avoid loss of intracellular GSH due to ischemia-induced formation of GSSG and its subsequent efflux from the liver (6), and to minimize hydrolysis of high-energy phosphagens (18). Degradation of GSH induced by γ -GT upon thawing of tissue prior to PCA extraction appears to be negligible since no ^{13}C -labeled cys-gly was detected in extracts. Furthermore, PCA is known to inactivate γ -GT (42). In vitro formation of protein-mixed disulfides (PSSG), which would be lost in the pellet, is reported to be insignificant in PCA extracts of

desanguinated liver (43), but occurs extensively in blood due to a free radical reaction of oxygen with iron from heme (44). Oxidation of GSH to GSSG was shown to require heme-bound iron, which is released from hemoglobin within seconds after addition of PCA (44). When, as in the current study, blood-containing tissue is pulverized under liquid nitrogen, hemoglobin-derived heme is mixed thoroughly with tissue and thus will react not only with plasma-derived GSH but also with (previously) intracellular GSH to form GSSG and subsequently PSSG. Such formation of PSSG from intracellular GSH, and its subsequent loss in the pellet, may explain the reduced GSH-to-serine PAR in extracts.

In intact tissue the proportion of GSH present as PSSG depends on the GSH-to-GSSG ratio; under physiological conditions wherein the GSH-to-GSSG ratio exceeds 100, it amounts to less than 1% of the total intracellular GSH pool (36,45). The presence of significant amounts of PSSG *in vivo* (reaction 4 in Fig. 6) would have resulted in a broadening at the base of the GSH resonance (46). As no GSSG was detected in freshly prepared hepatic extracts, it can be reasonably assumed that the amount of PSSG during acquisition of *in vivo* spectra was negligible.

Although GSH synthesis occurs only in the cytosol, mitochondria contain 15–20% of the intracellular GSH pool (4,47). Cytosolic-mitochondrial GSH exchange (reaction 5 in Fig. 6) occurs through both a high- and a low-affinity mitochondrial GSH transporter (48,49). Under physiologic conditions, i.e., when the cytoplasmic GSH is not depleted, the exchange of GSH is rapid (48). Hence, we assume that in the current study the mitochondrial [2-¹³C-glycyl]GSH pool was in equilibrium with the cytosolic pool. However, whether that mitochondrial pool is visible *in vivo* ¹³C NMR remains to be determined. In previous ¹³C NMR studies of cultured cells (50), perfused liver (34,51), excised lens (46), and intact brain (33,52) no data have been reported on the visibility of ¹³C-labeled GSH in cellular organelles.

Kinetics of NMR-Detectable Metabolites

The analysis of hepatic GSH kinetics in the current study is based on the fact that glycine is not a rate-limiting substrate in GSH synthesis. GSH synthetase operates near V_{max} for glycine and well below the K_m for γ -glu-cys when concentrations are in the physiologic range (36,53). Therefore, it is unlikely that increases in glycine levels over the course of the experiment affect the rate of GSH synthetase. The fact that GSH synthetase is not rate-limiting was a major reason for monitoring ¹³C-glycine rather than one of the other two amino acid candidates, cysteine and glutamate. (Compare reaction 3 with reaction 2 in Fig. 6). Our kinetic analysis is further based on the assumptions that 1) hepatic glycine is in rapid equilibrium with blood glycine, 2) glycine has a high extraction ratio, and 3) it is distributed homogeneously (“well stirred”) across the liver. Under these circumstances, blood and highly perfused organs such as the liver may be treated kinetically as a common homogeneous unit generally referred to as the “central compartment.” Kinetic homogeneity does not necessarily mean that the drug (in this case glycine) concentrations in all tissues of the central compartment at any

given time are the same. However, it does assume that any change that occurs in the plasma level is quantitatively reflected in the central compartment tissue level (29). Experimental studies (37) suggest that indeed plasma glycine is in rapid distribution equilibrium with hepatic glycine. Kinetically, the relationship between glycine and GSH is analogous to that of an intravenously infused drug (glycine) with a relatively short half-life and its metabolite (GSH) with a relatively long half-life. According to commonly accepted pharmacokinetic rules (54), in such a situation the initial non-steady state of drug concentration (glycine isotopic enrichment) may be neglected when assessing the kinetics of the metabolite (¹³C-GSH isotope). As the half-life of glycine is much shorter (37,39) than that of GSH (by about a factor of 6) (37), the initial non-steady state of glycine isotopic enrichment supposedly has very little effect on GSH isotope enrichment. Therefore, a monoexponential fit should provide a reasonable estimate of GSH kinetics (54). The results of our kinetic analysis of GSH turnover rates are corroborated by their similarity to previously reported GSH kinetic data (36,55,56).

Analysis of hepatic extracts demonstrated that fractional isotope enrichment of ¹³C had reached 81% in glycine and 55% in GSH after 4 h of 2-¹³C-glycine infusion. FE values obtained in extracts after 1 and 2 h of 2-¹³C-glycine infusion suggest that FE of glycine, but not of GSH, had reached a steady state. This is supported by kinetic analysis of the *in vivo* data, which suggests that glycine FE reaches steady state after 2 h, but that about 11 h of 2-¹³C-glycine infusion would be required for GSH FE to reach steady state. As reported previously, in rats infused with [U-¹⁴C]glycine, plasma and hepatic concentrations of glycine had reached steady state within 2 h, the first time-point obtained (39). The fact that FE values of glycine did not reach 100% suggests that the intracellular glycine pool is in exchange with another compartment, most likely unlabeled proteins (Fig. 6). Under experimental conditions similar to ours, in rats infused with [U-¹⁴C]glycine, 36% of their total protein pool was replaced per day (39). Intestinal contents could provide an additional source of unlabeled glycine.

Turnover rates of GSH and glycine were estimated from the peak areas of *in vivo* ¹³C spectra obtained serially over a period of 4 h and after conversion of *in vivo* PARs to FE values. The conversion was based on FE values determined experimentally using high-resolution NMR analysis of hepatic extracts obtained at the end of each *in vivo* experiment. FE values at 1 and 2 h derived from *in vivo* PARs did not differ significantly from those determined experimentally in hepatic extracts at 1 and 2 h, respectively, suggesting that the FE values estimated from *in vivo* PARs were accurate.

The average GSH turnover rate in the current study was 0.32 h⁻¹ ($t_{1/2}$ of 2.2 h), which is consistent with the turnover rate reported previously in healthy Sprague-Dawley rats. In the reported studies, the turnover rate calculated from the fractional decrease of GSH after intravenous injection of radiolabeled amino acid precursors ranged from 0.2 h⁻¹ ($t_{1/2}$ = 3.6 h) to 0.4 h⁻¹ ($t_{1/2}$ = 1.6 h) in the fed and fasted state, respectively (55), and from 0.1 h⁻¹ ($t_{1/2}$ = 5.8 h) to 0.5 h⁻¹ ($t_{1/2}$ = 1.3 h) in 24- and 6-week-old rats (56), respectively. The rate of GSH synthesis depends on

γ -glutamylcysteinyl synthetase (GCS) levels, allosteric regulation of GCS, and the bioavailability of cysteine (reaction 2, Fig. 6) (36). Together with cell efflux, redox cycling of GSH, and conjugation of electrophilic agents (Fig. 6) (1,57), the rate of GSH synthesis determines the intracellular steady-state concentration of GSH. These processes are affected by age, sex, nutritional status, signaling pathways elicited by surgery-induced catecholamines, and by xenobiotic challenge (6,57). In the current study, a relatively fast turnover rate would be expected as the rats were young and presumably were exposed to high levels of catecholamines due to surgical implantation of the NMR coil (57). The average turnover rate of glycine in the current study was 1.7 h^{-1} ($t_{1/2} = 25 \text{ min}$), and is similar to previously reported values in rabbits (1.8 to 6.0 h^{-1} ($t_{1/2} = 7$ to 23 min) (58)) obtained following an intravenous bolus of ^{15}N -glycine.

^{13}C -Glycine is incorporated into GSH either through de novo GSH synthesis or through exchange via GSH synthetase (reaction 3, Fig. 6) (59). This exchange is inhibited by both glucose and ATP (59). Since in the current study ATP levels were not depleted as determined by ^{31}P NMR, and because glucose was infused throughout the experiment, the increasing ^{13}C -labeling of GSH probably represents mainly de novo synthesis. GSH synthesis varies across the liver. It is largest in the pericentral region of the acinus (60) and is nearly two orders of magnitude smaller on a per cell basis in nonparenchymal cells (61). Therefore, the majority of in vivo GSH signal probably arises from parenchymal cells in the pericentral region.

CONCLUSIONS

A novel in vivo $^{13}\text{C}/^{31}\text{P}$ NMR animal model in conjunction with hepatic extracts has been applied for the first time to monitor GSH in the liver of intact animals. ^{13}C -labeled glycine was used to enrich ^{13}C in GSH because glycine, unlike cysteine or glutamate, does not affect GSH homeostasis (36), is not systemically toxic, and is an order of magnitude less costly than both cysteine and glutamate. No changes in hepatic bioenergetics or intracellular pH were detected during the course of the experiment. The procedure has potential for use in clinical studies wherein GSH metabolism may be affected.

ACKNOWLEDGMENTS

We are grateful to the University of California Toxic Substances Research and Teaching Program for support of this project, and the UCSF Research Evaluation Allocation Committee for support of the ^1H feasibility studies. J.M.M. received support in the final phase of this project from an NIH IRTA fellowship, an NIH NRSA fellowship (F32 DK09713), an NIH grant (R01 DK52851; Lola M. Reid, P.I.), and from the Johns Hopkins Center for Alternatives to Animal Testing. We are very grateful to Dr. Michael Gamcsik for consultation in the determination of GSH FE. We thank Drs. Lee-Hong Chang and Eugene DeRose for technical advice. J.M.M. was awarded the UCSF Eino Nelsen Prize for distinguished thesis research in pharmaceutical chemistry for the study described herein.

REFERENCES

1. Meister A. Metabolism and function of glutathione. In: Dolphin D, Poulson R, Avramovic O, editors. Coenzymes and cofactors. Vol. III. Glutathione: chemical, biochemical, and medical aspects. Part A. New York: John Wiley & Sons; 1989. p 367–474.
2. Sen CK. Redox signaling and the emerging therapeutic potential of thiol antioxidants. *Biochem Pharmacol* 1998;55:1747–1758.
3. Schafer FQ, Buettner GR. Redox environment of the cell as viewed through the redox state of the glutathione disulfide/glutathione couple. *Free Radic Biol Med* 2001;30:1191–1212.
4. Fernandez-Checa JC, Kaplowitz N, Garcia-Ruiz C, Colell A. Mitochondrial glutathione: importance and transport. *Semin Liver Dis* 1998;18:389–401.
5. Hall AG. Review: the role of glutathione in the regulation of apoptosis. *Eur J Clin Invest* 1999;29:238–245.
6. Lu SC. Regulation of hepatic glutathione synthesis. *Semin Liver Dis* 1998;18:331–343.
7. Ookhtens M, Kaplowitz N. Role of the liver in interorgan homeostasis of glutathione and cyst(e)ine. *Semin Liver Dis* 1998;18:313–329.
8. Keppler D, Leier I, Jedlitschky G, Konig J. ATP-dependent transport of glutathione S-conjugates by the multidrug resistance protein MRP1 and its apical isoform MRP2. *Chem-Biol Interact* 1998;111–112:153–161.
9. Hanigan MH. Gamma-glutamyl transpeptidase, a glutathionase: its expression and function in carcinogenesis. *Chem-Biol Interact* 1998;111–112:333–342.
10. Colvin OM, Friedman HS, Gamcsik MP, Fenselau C, Hilton J. Role of glutathione in cellular resistance to alkylating agents. *Adv Enzyme Regul* 1993;33:19–26.
11. Fan TW, Higashi RM. Reproducible nuclear magnetic resonance surface coil fabrication by combining computer-aided design and a photoresist process. *Anal Chem* 1989;61:636–638.
12. Chang L-H, Chew WM, Weinstein PR, James TL. A balanced-match double-tuned probe for in vivo ^1H and ^{31}P NMR. *J Magn Reson* 1987;72:168–172.
13. Koretsky AP, Wang S, Murphy-Boesch J, Klein MP, James TL, Weiner MW. ^{31}P NMR spectroscopy of rat organs, *in situ*, using chronically implanted radiofrequency coils. *Proc Natl Acad Sci USA* 1983;80:7491–7495.
14. Fan TW, Higashi RM, Lane AN, Jardetzky O. Combined use of ^1H -NMR and GC-MS for metabolite monitoring and in vivo ^1H -NMR assignments. *Biochim Biophys Acta* 1986;882:154–167.
15. Latner KH, Led JJ, Grant DM. Deuterium isotope effects on carbon-13 chemical shifts in amino acids and dipeptides. *J Magn Reson* 1975;20:530–534.
16. Macdonald JM, LeBlanc DA, Haas AL, London RE. An NMR analysis of the reaction of ubiquitin with [acetyl- ^{13}C]aspirin. *Biochem Pharmacol* 1999;57:1233–1244.
17. Bottomley PA, Roemer PB. Homogeneous tissue model estimates of RF power deposition in human NMR studies. Local elevations predicted in surface coil decoupling. *Ann NY Acad Sci* 1992;649:144–159.
18. Malloy CR, Cunningham CC, Radda GK. The metabolic state of the rat liver in vivo measured by ^{31}P -NMR spectroscopy. *Biochim Biophys Acta* 1986;885:1–11.
19. Macdonald JM, Grillo M, Schmidlin O, Tajiri DT, James TL. NMR spectroscopy and MRI investigation of a potential bioartificial liver. *NMR Biomed* 1998;11:55–66.
20. Endre ZH, Kuchel PW. Viscosity of concentrated solutions and of human erythrocyte cytoplasm determined from NMR measurement of molecular correlation times. The dependence of viscosity on cell volume. *Biophys Chem* 1986;24:337–356.
21. Seo Y, Murakami M, Watari H, Imai Y, Yoshizaki K, Nishikawa H, Morimoto T. Intracellular pH determination by a ^{31}P -NMR technique. The second dissociation constant of phosphoric acid in a biological system. *J Biochem* 1983;94:729–734.
22. Rothman DL, Behar KL, Hetherington HP, den Hollander JA, Bendall MR, Petroff OA, Shulman RG. ^1H -Observe/ ^{13}C -decouple spectroscopic measurements of lactate and glutamate in the rat brain in vivo. *Proc Natl Acad Sci USA* 1985;82:1633–1637.
23. Gamcsik MP. ^{13}C -Isotopic enrichment of glutathione in cell extracts determined by nuclear magnetic resonance spectroscopy. *Anal Biochem* 1999;266:58–65.
24. Rabenstein DL, Keire DA. Nuclear magnetic resonance spectroscopy of glutathione. In: Dolphin D, Poulson R, Avramovic O, editors. Coenzymes and cofactors. Vol. III. Glutathione: chemical, biochemical, and medical aspects. Part A. New York: John Wiley & Sons; 1989. p 67–102.

25. Vita JA, Frei B, Holbrook M, Gokce N, Leaf C, Keane Jr JF. L-2-Oxothiazolidine-4-carboxylic acid reverses endothelial dysfunction in patients with coronary artery disease. *J Clin Invest* 1998;101:1408–1414.
26. Olney JW, Zorumski C, Price MT, Labruyere J. L-cysteine, a bicarbonate-sensitive endogenous excitotoxin. *Science* 1990;248:596–599.
27. Banks MF, Stipanuk MH. The utilization of N-acetylcysteine and 2-oxothiazolidine-4-carboxylate by rat hepatocytes is limited by their rate of uptake and conversion to cysteine. *J Nutr* 1994;124:378–87.
28. Shungu DC, Bhujwala ZM, Li S-J, Rose LM, Wehrle JP, Glickson JD. Determination of absolute phosphate metabolite concentrations in RIF-1 tumors in vivo by ^{31}P - ^1H - ^2H NMR spectroscopy using water as an internal intensity reference. *Magn Reson Med* 1992;28:105–121.
29. Gibaldi M, Perrier D. *Pharmacokinetics*, 2nd ed. New York: Marcel Dekker Inc; 1982.
30. London RE. ^{13}C NMR spectroscopy. In: Levy GC, editor. *NMR spectroscopy: new methods and applications*. Washington, D.C.: American Chemical Society; 1982:119–142.
31. Anderson ME. Glutathione: an overview of biosynthesis and modulation. *Chem-Biol Interact* 1998;111–112:1–14.
32. Brown FF, Campbell ID, Kuchel PW, Rabenstein DC. Human erythrocyte metabolism studies by ^1H spin echo NMR. *FEBS Lett* 1977;82:12–16.
33. Trabesinger AH, Weber OM, Duc CO, Boesiger P. Detection of glutathione in the human brain in vivo by means of double quantum coherence filtering. *Magn Reson Med* 1999;42:283–289.
34. Cohen SM. Effects of insulin on perfused liver from streptozotocin-diabetic and untreated rats: ^{13}C NMR assay of pyruvate kinase flux. *Biochemistry* 1987;26:573–580.
35. Nicholson JK, Timbrell JA, Bales JR, Sadler PJ. A high resolution proton nuclear magnetic resonance approach to the study of hepatocyte and drug metabolism. Application to acetaminophen. *Mol Pharmacol* 1985;27:634–643.
36. Griffith OW, Mulcahy RT. The enzymes of glutathione synthesis: gamma-glutamylcysteine synthetase. *Adv Enzymol Relat Areas Mol Biol* 1999;73:209–267.
37. Jahoor F, Wykes LJ, Reeds PJ, Henry JF, del Rosario MP, Frazer ME. Protein-deficient pigs cannot maintain reduced glutathione homeostasis when subjected to the stress of inflammation. *J Nutr* 1995;125:1462–1472.
38. Groszmann D, Franchis R. Portal hypertension. In: Schiff ER, Sorrell MF, Maddrey WC, editors. *Shiff's diseases of the liver*, 8th ed. Philadelphia: Lippincott Williams & Wilkins; 1999. p 387–442.
39. Fern EB, Garlick PJ. The specific radioactivity of the tissue free amino acid pool as a basis for measuring the rate of protein synthesis in the rat in vivo. *Biochem J* 1974;142:413–419.
40. Snell K. Enzymes of serine metabolism in normal, developing and neoplastic rat tissues. *Adv Enzyme Regul* 1984;22:325–400.
41. Gadian D. *Nuclear magnetic resonance and its application to living systems*. New York: Oxford University Press. 1989.
42. Roberts JC, Francetic DJ. The importance of sample preparation and storage in glutathione analysis. *Anal Biochem* 1993;211:183–187.
43. Andersen ME. Enzymatic and chemical methods for the determination of glutathione. In: Dolphin D, Poulson R, Avramovic O, editors. *Coenzymes and cofactors*. Vol. III. Glutathione: chemical, biochemical, and medical aspects. Part A. New York: John Wiley & Sons; 1989. p 339–366.
44. Gallemann D, Eyer P. On the mechanism of hydrogen peroxide formation during precipitation of hemoglobin with perchloric acid. *Biol Chem Hoppe-Seyler* 1990;371:881–887.
45. Gilbert HF. Molecular and cellular aspects of thiol-disulfide exchange. *Adv Enzymol Relat Areas Mol Biol* 1990;63:69–172.
46. Willis JA, Schleich T. ^{13}C -NMR spectroscopic studies of 2-mercaptoethanol-stimulated glutathione synthesis in the intact ocular lens. *Biochim Biophys Acta* 1995;1265:1–7.
47. Griffith OW, Meister A. Origin and turnover of mitochondrial glutathione. *Proc Natl Acad Sci USA* 1985;82:4668–4672.
48. Martensson J, Lai JC, Meister A. High-affinity transport of glutathione is part of a multicomponent system essential for mitochondrial function. *Proc Natl Acad Sci USA* 1990;87:7185–7189.
49. Lash LH. Intracellular distribution of thiols and disulfides: assay of mitochondrial glutathione transport. *Methods Enzymol* 1995;252:14–26.
50. Gamcsik MP, Millis KK, Colvin OM. Noninvasive detection of elevated glutathione levels in MCF-7 cells resistant to 4-hydroperoxycyclophosphamide. *Cancer Res* 1995;55:2012–2016.
51. Cohen SM. ^{13}C NMR study of effects of fasting and diabetes on the metabolism of pyruvate in the tricarboxylic acid cycle and the utilization of pyruvate and ethanol in lipogenesis in perfused rat liver. *Biochemistry* 1987;26:581–589.
52. Hanstock DL, Brown K, Boisvert DP. Feasibility of in vivo glutathione measurement in brain and tumor tissue by 3D-ISIS localized NMR spectroscopy. In: *Proceedings of the 10th Annual Meeting of SMRM*, San Francisco, 1991. p 598.
53. Oppenheimer L, Wellner VP, Griffith OW, Meister O. Glutathione synthetase: purification from rat kidney and mapping of the substrate binding sites. *J Biol Chem* 1979;254:5184–5190.
54. Rowland M, Tozer TN. *Clinical pharmacokinetics: concepts and applications*, 2nd ed. Philadelphia: Lea and Febiger; 1989. p 546.
55. Lauterburg BH, Mitchell JR. Regulation of hepatic glutathione turnover in rats in vivo and evidence for kinetic homogeneity of the hepatic glutathione pool. *J Clin Invest* 1981;67:1415–1424.
56. Lauterburg BH, Vaishnav Y, Stillwell WG, Mitchell JR. The effects of age and glutathione depletion on hepatic glutathione turnover in vivo determined by acetaminophen probe analysis. *J Pharmacol Exp Ther* 1980;213:54–58.
57. Kaplowitz N, Aw TY, Ookhtens M. The regulation of hepatic glutathione. *Ann Rev Pharmacol Toxicity* 1985;25:715–744.
58. Nissim I, Lapidot A. Plasma amino acid turnover rates and pools in rabbits: in vivo studies using stable isotopes. *Am J Physiol* 1979;237:E418–E427.
59. York MJ, Kuchel PW, Chapman BE, Jones AJ. Incorporation of labelled glycine into reduced glutathione of intact human erythrocytes by enzyme-catalysed exchange. A nuclear-magnetic-resonance study. *Biochem J* 1982;207:65–72.
60. Jungermann K. Functional heterogeneity of periportal and perivenous hepatocytes. *Enzyme* 1986;35:161–180.
61. DeLeve LD. Glutathione defense in non-parenchymal cells. *Semin Liver Dis* 1998;18:403–413.